Chia-Chiang Ho received the B.S. degree in computer science and information engineering from National Taiwan University, Taipei, Taiwan, in 1996. Currently, he is a Ph. D student in the same department. His research interest includes video coding, video streaming and multimedia system design.

Jin-Hau Kuo received the B.S. degree in information and computer engineering from Tatung University, Taipei, Taiwan, in 1997. He is currently a Ph.D. student in the department of computer science and information engineering, National Taiwan University. His current research interests include data compression, digital image processing, content-based retrieval, code optimization, and multimedia systems.

Ja-Ling Wu received the B.S. degree in electronic engineering from TamKang University, Tamshoei, Taiwan, R.O.C. in 1979, and the M.S. and Ph.D degree in electrical engineering from Tatung Institue of Technology, Taipei, Taiwan, in 1981 and 1986, respectively. From 1986 to 1987, he was an Associate professor of the Electrical Engineering Department at Tatung Institute of Technology, Taipei, Taiwan. Since 1987, he has been with the Department of Computer Science and Information Engineering, National Taiwan University, where he is presently a Professor. He was also the Head of the Department of Information Engineering, National Chi Nan University, Puli, Taiwan, from Aug. 1996 to July. 1998.

Prof. Wu was the recipient of the 1989 Outstanding Youth Medal of the Republic of China, the Outstanding Research Award sponsored by the National Science Council, from 1987 to 1992, and the Excellent Research Award from NSC, 1999.

Prof. Wu has published more than 200 journal and conference papers. His research interests include algorithm design for DSP, data compression, digital watermarking techniques and multimedia systems.

A Multi-Loop Voltage-Feedback Filterless Class-D Switching Audio Amplifier using Unipolar Pulse-Width-Modulation

Alejandro R. Oliva, Simon S. Ang and Thuy V. Vo

Abstract — *Voltage feedback is frequently used in class-D switching audio power amplifiers. This paper discusses the design and implementation of a low-cost filterless class-D, unipolar pulse-width modulation switching audio amplifier having a multi-loop voltage feedback scheme. Classical frequency-compensation techniques are used to design and stabilize the three voltage feedback loops implemented in this application. This design method proves to be a cost-effective solution for designing high-fidelity (hi-fi) audio amplifiers. The cost is reduced because no output filter is used, the required switching frequency is half of the one needed if bipolar PWM was used, and no current sensor is needed for feedback purposes. The output impedance is extremely low due to the reduction of the successive voltage loops, making the amplifier less load dependent. Simulation results show that a total harmonic distortion (THD) of 0.005% can be achieved using this topology, as well as a flat frequency response, free of phase distortion in the audio band. Experimental results show the feasibility of this control scheme, since a THD of 0.05% was achieved with a laboratory prototyped amplifier. A comparison of the performance of this audio amplifier with that of some commercial class-D audio amplifiers, reveals that our design can seriously compete with some of the ICs leading the market at a lower cost[1].*

Index Terms — **Amplifier distortion, Audio amplifier, Class-D amplifier, Feedback amplifiers, Power amplifiers, Switching amplifiers.**

I. INTRODUCTION

CLASS-D amplifiers are becoming the workhorses for audio amplifiers power stages. The principal reason is the high efficiency that can be achieved using this topology. However, distortions due to the nonlinear nature of the switching stage are the main drawback for this amplifier topology.

Many different approaches have been studied to overcome the inherent nonlinearity in the class-D amplifier topology. Jung et al [1] reported a parallel combination of a linear amplifier and a switching amplifier that yielded a minimum THD of 0.005% near 20 kHz. However, the reported THD increased monotonically to 0.1% at 20 Hz. Himmelstoss et al [2] worked on a series combination of two switching amplifiers. Nevertheless, no experimental THD results were given. Ertl et al [3] also proposed some similar concepts in the implementation of class-D amplifiers.

A great effort has been made to linearize the class-D amplifier, resulting in a switching stage free of distortion; such is the case of PEDEC, a digital feedback scheme proposed by Nielsen [4]. The ZePoC, by Streitenberger [5], is an amazing algorithm that solves the demodulation problem in the class-D amplifier, but as many others; it requires high switching frequencies and/or a large computational power. These requirements may contribute to the degradation of the overall efficiency and to a cost increase.

Some very sophisticated class-D switching audio amplifiers are gaining in the high-end audio amplifier market, using different modulation techniques, for example there is one analog-input class-D audio amplifier with feedback that uses sigma-delta modulation switching at 2.82 MHz, instead of PWM [6]. Others are fully digital [7], with an open-loop power D/A converter capable of driving speakers directly, without having any analog circuitry after D/A conversion. These amplifiers have an astounding performance at the expense of the PWM to switch over 90 MHz.

There is a need for low cost and high efficiency audio amplifiers; the main targets are the so-called *information appliances* [8]. A possible implementation would eliminate the output low pass filter (LPF) (to reduce costs and volume) and improve the output stage by a low-cost linearization of the class-D topology. Trying to satisfy this need, we propose the use of a (multi-loop) negative feedback scheme, a very well known design technique to most audio amplifier designers, to implement a hi-fi switching audio amplifier. Multi-loop feedback is not new to audio amplifier; Anderskouv et. al. published many papers on feedback in class-D audio amplifiers including multi-loops [9]. They reported a current-voltage feedback topology with low THD up to 200 Hz, and a linear increase up to 0.1% after that. A similar approach was covered in [10], a current-voltage feedback was applied to a class-D audio amplifier with an output filter. Chang et al tested a voltage-feedback low-power class-D audio amplifier with an output filter and they reported a satisfactory THD reduction [11]. The LPF used in the above implementations is responsible for two major problems. Firstly, it decreases the amplifier control over the speaker, especially at high frequencies where the amplifier frequency transfer becomes load dependent. Secondly, the filter components suffer from non-linearities [12]. Thus, a good LPF is one of the most expensive components of the audio amplifier.

In this paper, we describe the implementation of a *multi-loop voltage feedback* class-D switching audio amplifier, *without an output filter*, using a *unipolar PWM* scheme [13][2]. Even though the *unipolar* PWM scheme seems to be very attractive for this type of applications, because it effectively

[2] Also called double-sided BD PWM [9].

doubles the switching frequency of the class-D audio amplifier, to our knowledge there are just a few papers in this area [4], [9], [15]. However, an output filter was used in [4], [9], [15]. The multiple voltage feedback loops serve to bring the THD down to the required level, while contributing to an extremely low output impedance.

PWM was chosen among various modulation techniques because it *has been found to be the best suited modulation technique* for conveying analogue power in a digital signal since it inherently uses the fewest edges per unit time. Other techniques, such as in *bitstream* converters, employing high oversampling (256x) and delta sigma modulation to convert digital audio to analogue power, all require a higher output pulse rate which introduces more noise and reduces the switching efficiency, limiting resolution and maximum power output [4].

Conventional audio amplifiers are usually analog amplifiers with a class-B (or AB) power stage. The main problem of this power stage topology is the crossover distortion due to the nonlinearities inherently present in the output power transistors. In these amplifiers, a negative feedback technique is usually employed to linearize the transfer characteristics, thus reducing their distortions [16]. This situation is illustrated in Figure 1, where $A_2(s)$ represents a linear power stage whose nonlinearities are modeled as an external distortion source, e_2. Normally, the power stage is designed with a gain of 1. A large gain, $A_1(s)$, is usually employed in the stage before $A_2(s)$. Negative feedback is then applied to reduce the nonlinear distortion with a concomitant decrease in gain. Frequency compensation is added, as needed, to stabilize the loop. It can be shown that the distortion (as well as the output impedance) is reduced by $(1+\beta A)$, where β is the feedback factor and A is the composite open-loop gain of the amplifier. Thus, the larger the product of βA, the smaller is the output distortion [16]. If an ideal amplifier with an infinite gain were used to implement A_1, the output distortion would be reduced to zero. However, in practice, it is not advisable to use the large open-loop gain of an operational amplifier circuit as the gain stage. The main reason is that the *slew-rate* is unaffected by feedback and depends on the physical limitations of the circuit components; thus, limiting the maximum rate of growth of the signal. Hence, there is a maximum amplitude that the amplifier can produce, and that amplitude is a function of frequency. Consequently, *maximum sinusoidal power is obtainable at frequencies below the open-loop frequency response of the power stage* [18]. Thus, only one feedback loop may not be enough to reduce the distortion below the desired level. As such, feedback loop nesting may be used to further reduce distortions. One could, ideally, nest as many loops as desired, until the pursued signal-quality is achieved. This is, of course, limited by the quality and linearity of the components used in the feedback block.

If we think of a class-D amplifier as a non-linear amplifier, we can expect the use of a negative feedback can help to reduce signal distortion. Moreover, if we apply a second feedback loop to a closed-loop amplifier, we would expect its signal distortion to be further reduced. In this paper, the feasibility of nesting three voltage loops is explored. Our experimental data show
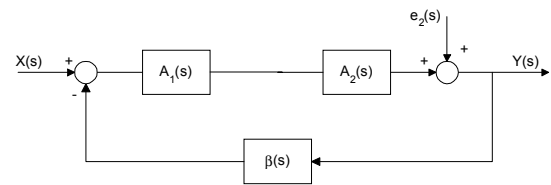

Figure 1   Distortion reduction by negative feedback.

that with this scheme of nesting three loops to a class-D switching audio amplifier, hi-fi THD levels can be achieved with only a very small degradation in its efficiency. We also illustrate how a switching audio amplifier with a low THD can be designed using simple techniques available in the toolbox of any audio amplifier designer. This approach also has the advantage of being easily implemented in integrated circuit form, and it does not require a current sensor.

In designing class-D switching audio amplifier, its complexity can be reduced considerably without an output filter. This method also reduces the overall cost, since operational amplifiers, resistors and small capacitors can replace the output filter more efficiently in integrated circuit form. As stated in [19], the second order output filter for a class-D audio amplifier is 30% of the amplifier's cost. If a speaker that is highly inductive at the switching frequency and properly designed to support the PWM waveform is used without any LPF, then the speaker's dynamics in combination with the human ears frequency response will reconstruct the audio waveform. Nevertheless, this topology is restricted for those applications where the amplifier can be kept close to the voice coil in a shielded environment, like in shielded powered speakers, to maintain EMI within admissible levels.

II.   DESIGN

This section describes the procedures for designing our amplifier. Only an intuitive design approach is discussed. The background knowledge for frequency compensation can be found in many textbooks, such as [17].

A.   Power stage design

The power stage is a typical H-bridge topology, where the gates of the power MOSFETs can be driven independently, allowing a unipolar-PWM scheme to be employed [13]. The MOSFETs used for this implementation were driven by MOSFET drivers with additional logics to introduce a dead time of 100 ns. As shown in [20], the dead time is the main source of distortion in class-D audio amplifiers. Accordingly, we set the upper limit for the dead time to 5% of the switching period.

B.   PWM modulator design

The PWM modulator gives the desired gain to the power stage. As discussed in various textbooks (such as [16]), the improvement in signal distortion by feedback is better when the power stage has a unity gain. Another consideration is that the slope of the triangular waveform determines the maximum slope of the audio signal being processed (or the error signal,

if feedback is applied). This leads to the choice of the PWM-modulator gain to be one.

For the unipolar-PWM modulator the triangular carrier is compared with the audio signal as well as the same signal shifted 180 degrees to yield the unipolar PWM signals.

The PWM modulator gain can be calculated as:

$$A(s) = \frac{V_{cc}}{V_{tri}} e^{-s t_d}$$

where V_{cc} is the voltage level of the output-stage power supply, V_{tri} is the peak amplitude of the triangle waveform and t_d is the time delay associated with all the switching devices. In the present design, we had to compromise the slew rate of the operational amplifiers and the available triangular source, thus we chose V_{cc} = 10 V and V_{tri} = 10 V. Therefore, the gain of the PWM modulation stage is 1 (or 0 dB). The delay of the switching block was measured from the analog input of the comparator to the load, yielding a value of 100 ns.

The main advantage of unipolar-PWM is that no spectral bins appear at the odd multiples of the switching frequency, and no multiples of the switching frequency are present. The first spectral bin that appears outside of the base-band corresponds to $2F_s$-f_o [13] [3]. *This essentially doubles the switching frequency*, moving the unwanted frequency components far away from the audio band; thus allowing the specifications of the LPF (if present) to be relaxed. A triangular carrier is preferred over a saw-tooth carrier due to its lower harmonic contents [15].

C. Modeling

It was necessary to obtain a linear model to perform the frequency-domain simulations in PSpice. PSpice does a small-signal approximation when simulating a frequency response; thus, it is not suitable to obtain the frequency response of a switching amplifier. In this case, the non-linear characteristic of the amplifier is due mainly to the switching actions, dead time, and time delays contributed by the control logic and the MOSFETs. This section shows the linear model and the time-delay block used for the design of the class-D audio amplifier.

1) Power stage model

Let us define the power stage as the system formed by the PWM-modulator and the H-bridge. This is obviously a non-linear system. Nevertheless, it can be modeled, as shown in Figure 2, as a linear subsystem A [21], a subsystem B, representing the time delay; and a distortion source δ, modeling the nonlinearities [22]. Subsystem A includes an ideal gain block to model the PWM modulator. Subsystem B is a time delay modeling the switching devices.
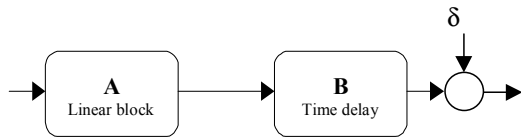

Figure 2 Linear model of the power stage.

[3] F_s is the switching frequency; f_o is the modulating signal frequency.

2) Linear design

The linear design will neglect the distortion source δ, and make use only of the linear block A to calculate the frequency compensation of the linearized amplifier by classical control techniques (Bode plots in this case). Once the phase margin is measured, the phase contribution due to the time delay (block B) is added to compute the approximated phase margin.

Figure 3 shows the single-ended block-diagram representation of the three-loop implementation. Starting with the inner loop, each loop was designed with the aid of PSpice simulations. The linear system was modeled in the frequency domain. The loop was frequency compensated, considering only the linear subsystem A. Then, the loop gain and phase were evaluated for stability. The phase shift due to the time delay at the frequency corresponding to the loop gain equal to 1 was calculated and added to the unity-gain phase to obtain the phase margin. This procedure gives a good approximation if a close estimation of the time delay can be made [22]. Once the frequency compensation is calculated, the results can be checked using time-domain simulations. Open-loop simulations using vendor Spice models showed a delay time of 100 ns from the comparator to the load, in agreement with the experimental measurements.
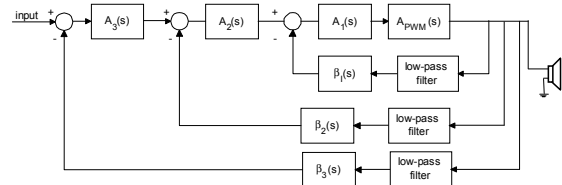

Figure 3 Block diagram representation of three nested loops.

3) Inner loop design

The design of the inner loop will only be discussed in detail. The design of the other two outer loops was performed using a similar approach. It is very important to include the speaker model when simulating the loop gain. This is because the stability of the amplifier is affected by the frequency response of the speaker due to its phase contribution. An inductive speaker is preferred, because it adds phase margin while reducing EMI emission. In addition, the speaker can be considered as a special case of a linear motor. Therefore, its current is proportional to the torque that produces the acoustic wave. A larger inductance would produce a smaller ripple in the current and thus, a smaller torque ripple. A larger inductance leads to a smaller amount of radiated ultrasonic noise.

From Figure 3, the open loop gain can be calculated as $A_1 \cdot A_0$; where $A_0 = A_{pwm} \cdot A$, and A is the gain of the error amplifier. In our case, A was set to 100 V/V. The feedback factor, β_1 was chosen as 1. A 72-kHz one-pole low-pass RC filter was inserted at the input of the sensing amplifier to avoid slew-rate distortion. Details of the circuit are given in the Appendix.

The uncompensated loop gain is displayed in Figure 4. The phase margin is negative; thus, a proper amount of frequency compensation is required.
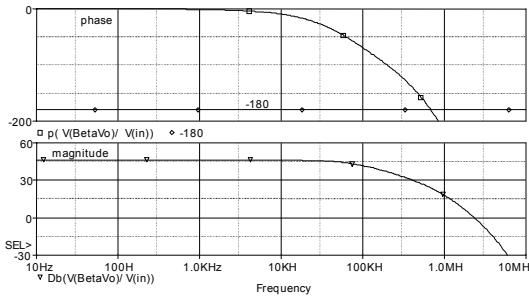
Figure 4   Uncompensated loop response of the inner loop.

4) Frequency compensation

The frequency compensation was implemented using a zero-pole active network after the error amplifier. The pole was located at 860 Hz while a zero at 36 kHz was chosen to cancel out the first pole of the uncompensated amplifier.

The compensated loop response is displayed in Figure 5, where the new unity-gain frequency of the loop response is situated at 329 kHz, with a phase margin of 65°. Since this phase margin was calculated from the linear model, the effect of the time delay must be added. The time delay contribution to the phase margin is:

$$PM = PM_{sim} - 360 * t_{delay} * f_{0db};$$ where PM_{sim} is the PM

obtained from the simulation, $t_{delay} = 100\,ns$ and f_{0db} is the unity-gain frequency obtained in the simulation.

The contribution of the time delay is approximately 12°. Hence, the phase margin is 65°-12° = 53°, yielding a stable amplifier response.
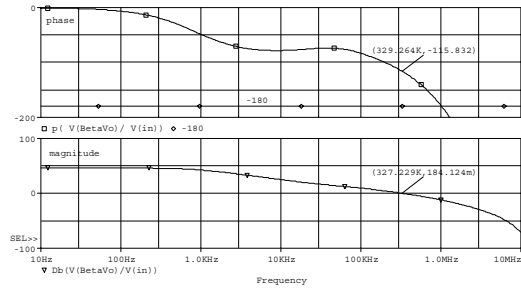

Figure 5   Compensated loop response of the inner loop.

5) Closed loop response

Figure 6 displays the closed loop response of the inner loop after applying the frequency compensation. Notice that the loop is stable and behaves as a second-order under-damped system, with a flat magnitude response up to 50 kHz.
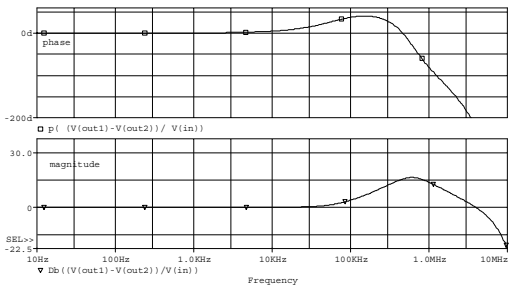

Figure 6   Closed loop response of the inner loop.

6) Second Voltage loop design

Similar to the inner loop, the second voltage loop was frequency compensated until the desired response was obtained, resulting in the closed-loop response shown in Figure 7, where the phase and magnitude remain flat up to 100 kHz.
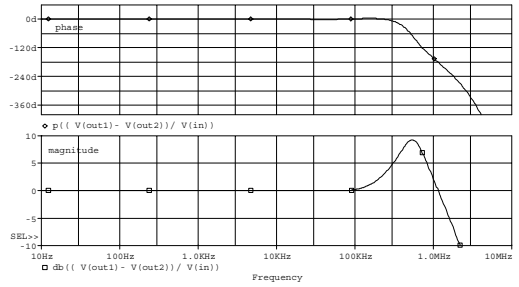

Figure 7   Closed loop response of the second loop.

7) Third Voltage feedback loop

Finally, the third voltage loop was frequency compensated using another zero-pole active network. The overall closed-loop response is shown in Figure 8. Note that the magnitude and phase responses start at DC and show a flat response up to 20 kHz. The phase contribution at 20 kHz is less than 1°, while the magnitude is attenuated for less than half a dB. It should be noted that a small phase contribution is desired within the audio band to avoid a significant phase distortion [23].
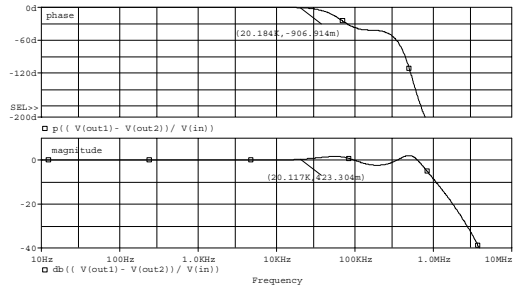

Figure 8 Overall closed-loop response.

8) Transient response

Time-domain simulations were performed using the calculated frequency compensations; but this time the nonlinear models for the switching devices were used. The simulations showed that the amplifier was stable and had a voltage THD of 0.0048% (only frequency components up to 20 kHz are considered) for a 10-V peak sinusoidal input signal of 1 kHz. With the exception of the 3rd harmonic (whose magnitude is $h_3 = 0.000035 * h_1$), all harmonic components have an amplitude smaller than $0.00002 * h_1$.

III. EXPERIMENTAL RESULTS

A laboratory prototype was constructed using surface-mount components for the power stage in order to minimize potential parasitic effects. The experimental results obtained from this board are discussed in this section.

A ±12-V power supply was used to power the signal stage while a single +10-V linear power supply was used for the

output stage. A speaker having a power rating of 40 W and a nominal impedance of 4 Ω was used. This speaker can be modeled as a combination of a 4-Ω resistor and a 400-μH inductor. To evaluate the amplifier responses, we replaced the speaker with an equivalent RL circuit. The switching frequency was chosen at 300 kHz, as a trade-off between the distortions that would be introduced by the dead time and the attenuations of the aliased frequency components. The quiescent current for the power stage was measured to be less than 10 mA. The quiescent current into the speaker is reduced by negative feedback.

THD+N characteristics were characterized using an audio analyzer. Audio standards [24] establish that the measurements of the hi-fi parameters of the audio amplifiers have to be performed within the audio band. As such, an active LPF with the required characteristics[4] [24] was connected in parallel with the load and measurements were taken at this output. We used the same experimental setup as described in [25], except that we replaced the passive RC filter by an active filter. The audio amplifier frequency responses are shown in Figure 9. The upper curve corresponds to its phase response and the lower trace corresponds to its magnitude response. As can be clearly seen, both the magnitude and phase responses are shaped by the frequency response of the active filter.
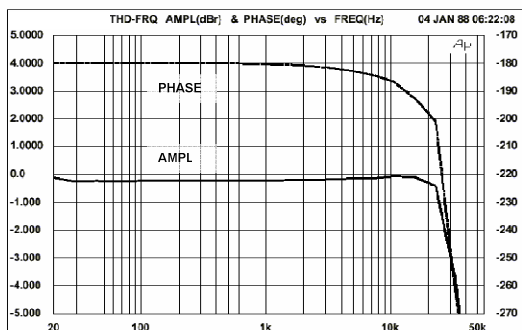

Figure 9 Frequency response of the class-D audio amplifier.

Figure 10 shows the frequency responses of the audio amplifier without the low-pass active filter at different speaker loads (trace *a* R_{load}=4 Ω; trace *b* R_{load}=2 Ω; trace *c* R_{load}=1 Ω). These measurements were taken using the RC LPF described by [25] instead of the active filter[5]. As expected, different speaker impedances affect the peaks of the magnitude responses; thus, affecting the phase margin. Nevertheless, the amplifier remained stable under these conditions.

THD+N of the prototyped amplifier under test are shown in Figure 11 through Figure 14, for the open-loop, one-loop, two-loop and three-loop configurations, respectively. Table I summarizes the measured THD+N for different feedback

configurations at 1 kHz using a 10 Vpp sinusoidal input. Notice that the curves are fairly flat up to 1 kHz but they start to increase after this frequency. Also, notice that every time a loop is added, the distortion reduces. As can be seen, there is not much of an improvement in THD+N in going from the two-loop configuration to the three-loop configuration. We atribute this to the background noise and the influence of the LPF used to make these measurements, which has a THD of 0.008% in the audio band.
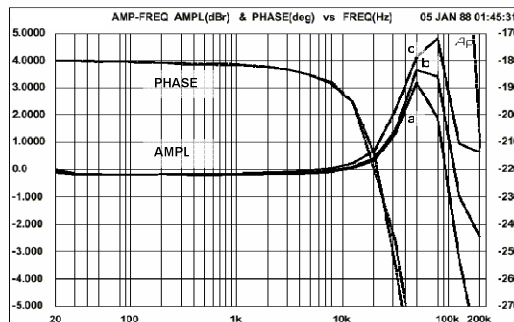

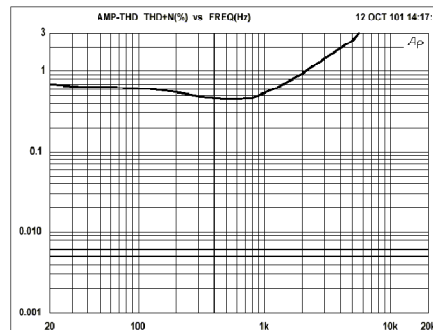**Figure 10 Frequency response of the audio amplifier for different speakers.**

Figure 11 THD+N vs. frequency for the open-loop amplifier.

THD+N versus frequency characteristics of the active LPF are shown in Figure 15. It can be noticed that the THD+N is about 0.009% below 1 kHz, but it starts to increase above 1 kHz, reaching 0.08% at 20 kHz. A dip in the THD+N is observed near the line frequency of 60 Hz that indicates the presence of line noise, probably due to a ground loop. This characteristic is obviously affecting the measurements and consequently, degrading the frequency responses of the audio amplifier. It is reasonable to expect that the measured high frequency characteristics of the audio amplifier would be similar to those of the LPF used in the measurements. Furthermore, the measured characteristics of the amplifier will never be better than those of the filter used for taking them. We can also attribute some distortion to the non-ideal sinusoidal input and triangular carrier; also, the linear power supply used as the main source contributes with noise in the audio band. A better performance would be expected if the

---

[4] Pass-band response deviation: ≤ ±0.1dB for 10Hz ≤ f ≤ 20kHz; stop-band attenuation: > 60dB for f > 24kHz.

[5] A low pass filter is required to take measurements with the audio analyzer, otherwise the input amplifier of the meter would saturate with a square wave input.

linear power supply would have been replaced by a switching power supply synchronized with the PWM clock [26].
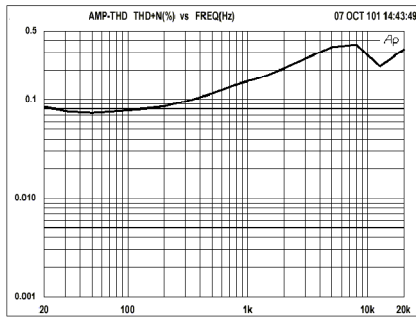

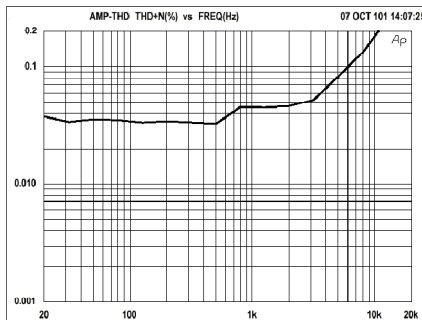**Figure 12 THD+N vs. frequency for one loop feedback.**

Figure 13 THD+N vs. frequency for two feedback loops.
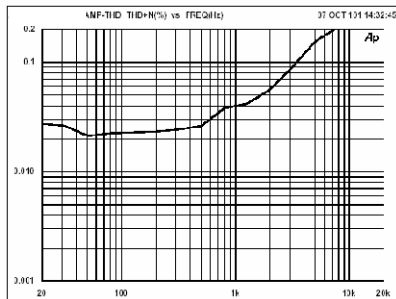

Figure 14 THD+N vs. frequency for three feedback loops.

A comparison of the performance of this audio amplifier with that of the commercial class-D audio amplifier shown in Figures 8 and 10 of [25], reveals that our design can seriously compete with one of the switching audio amplifiers ICs leading the market.

Table I Comparison of the audio amplifier THD+N measured at 1 kHz for different feedback configurations.

Feedback	Measured THD%	Expected THD% (1)
open loop	0.7	0.7
1 loop	0.14	0.015
2 loops	0.045	0.0003
3 loops	0.040	0.000006

(1) The expected HD% is calculated as the measured open loop THD divided by $(1+\beta A)=48$ of each loop.

IV. CONCLUSION

A filterless class-D switching audio amplifier was demonstrated with three voltage feedback loops. As shown in the simulation results, applying multiple voltage feedback loops can considerably reduce the THD of a class-D audio amplifier. Experimental results gave a 0.048% THD, which qualifies the audio amplifier to be in the hi-fi regime. Ground loops and a less than optimum layout probably contributed to a higher-than-expected THD in this prototyped audio amplifier. We attribute the discrepancies between the experimental and simulation results to the assumptions made in the model, including the non-ideal characteristic of the carrier waveform. It is our opinion that the LPF used for taking the measurements might contribute some distortion, degrading the measurements. A main drawback of this design is that the stability of the audio amplifier depends on the inductance of the speaker (as in any feedback amplifier). Thus, for a better audio quality, a high-inductive speaker and amplifier-speaker matching is recommended. Electromagnetic interference (EMI) radiation from the cables and speaker is another important consideration for the switching audio amplifier. However, these EMI radiations can be substantially reduced if the switching audio amplifier can be mounted very close to the load inside a shielded enclosure, as discussed in [19].

In addition to the THD and the output impedance reduction, the DC component across the speaker is also reduced by the action of the negative feedback.
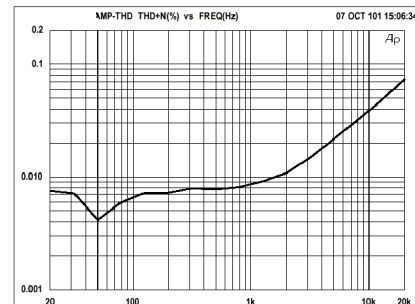

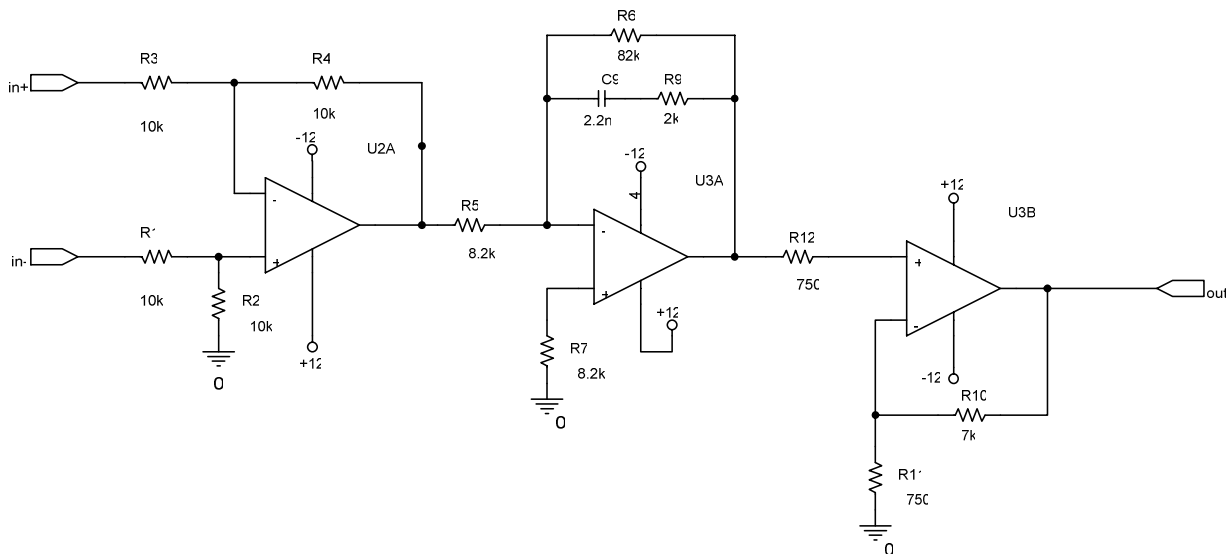**Figure 15 THD+N vs. frequency for the active low-pass filter.**

Figure 16   Error amplifier and direct gain of the first loop..

Figure 17   Feedback block of the first loop.

REFERENCES

[1]   N. S. Jung, J. H. Jeong, G. H. Cho, "High efficiency and hi fidelity analog/digital switching mixed-mode amplifier", *Electronics letters*, vol. 34, pp. 828-829, 1998.

[2]   F. A. Himmelstoss, K. H. Edelmoser, "High dynamic Class-D power amplifier", *IEEE Transactions on consumer electronics*, vol. 44, pp. 1329-1333, 1998.

[3]   H. Ertl, J. W. Kolar, F. C. Zach, "Basic Considerations and Topologies of Switched-Mode Assisted Linear Power Amplifiers", *IEEE Transactions on industrial electronics*, vol. 44, pp. 116-123, 1997.

[4]   Karsten Nielsen, "Audio Power Amplifier Techniques With Energy Efficient Power Conversion", Ph.D. Thesis, Department of Applied Electronics, Building 451 Technical University of Denmark, April 30, 1998.

[5]   M. Streitenberger, F. Felgenhauer, H. Bresch, W. Mathis, "Zero-Position Coding (ZePoC) - A Generalised Concept of Pulse-Length Modulated Signals and its Application to Class-D Audio Power Amplifiers", presented at the *110th Convention of the Audio Engineering Society*, May 12 - 15, 2001, Amsterdam, The Netherlands, Audio Eng. Soc. preprint, (5365), pp. 9

[6]   Michael Fremer, "Sharp SM-SX100 digital integrated amplifier", *Stereophile*, pp. 73-79, July 2000.

[7]   Lars Risbo, "Performance of an All-Digital Power Amplification System," presented at the *104th Convention of the Audio Engineering Society*, Preprint 4695, J. Audio Eng. Soc. (Abstracts), June 1998, vol. 46, p. 584.

[8]   Dennis Bohn, "Audio in a 1.5 Volt World", *Proceedings of the AES 18th International Conference: Audio for Information Appliances*, Burlingame, CA., pp. 52-65, March 16-18, 2001, Audio Engineering Society.

[9]   Niels Anderskouv, Karsten Nielsen & Michael A. E. Andersen, "High Fidelity Pulse Width Modulation Amplifiers based on Novel Double Loop Feedback Techniques", *100th AES Convention*, May 11-14, 1996, Copenhagen.

[10]   J. H. Jeong, G. H. Cho, "A high efficiency and wide bandwidth class D switching audio power amplifier with improved output stage and current mode control", *International Journal of Electronics*, 1997, vol. 82, pp. 533-554.

[11]   J. S. Chang, Bah Hwee Gwee, Yong Seng Lon, Meng Tong Tan, "A novel low-power low-voltage Class D amplifier with feedback for improving THD, power efficiency and gain linearity", *The 2001 IEEE International Symposium on Circuits and Systems*, ISCAS 2001, vol. 1, pp. 635-638.

[12]   Paul van der Hulst, André Veltman, René Groenenberg, "An asynchronous switching high-end power amplifier", Audio Engineering Society, *Presented at the 112th Convention*, May 10–13, 2002, Munich, Germany, Convention Paper 5503.

[13]   Ned Mohan, Tore M. Undeland and Robbins, P. William, *Power Electronics Converters, Applications, and Design,* John Wiley & Sons, ISBN 0471613428, 1995, pp. 215-217.